HHS Public Access

Author manuscript

Oncogene. Author manuscript; available in PMC 2020 October 14.

Published in final edited form as:

Oncogene. 2020 May ; 39(21): 4241–4256. doi:10.1038/s41388-020-1282-8.

Overexpression of TC-PTP in murine epidermis attenuates skin tumor formation

Mihwa Kim[1,#], **Liza D. Morales**[2,#], **Cheol Jung Lee**[1,#], **Serena A. Olivarez**[1], **Woo Jin Kim**[3], **Joselin Hernandez**[2], **Srinivas Mummidi**[2], **Christopher Jenkinson**[2], **Andrew T. Tsin**[1], **Ik-Soon Jang**[4], **Thomas J. Slaga**[5], **Dae Joon Kim**[*,1,2]

[1]Department of Molecular Science, School of Medicine, University of Texas Rio Grande Valley, Edinburg, TX;

[2]Department of Human Genetics, School of Medicine, University of Texas Rio Grande Valley, Edinburg, TX;

[3]School of Mathematical and Statistical Sciences, College of Sciences, University of Texas Rio Grande Valley, Edinburg, TX, USA;

[4]Division of Bioconvergence Analysis, Korea Basic Science Institute, Daejeon 305-333, Republic of Korea;

[5]Department of Pharmacology, School of Medicine, University of Texas Health Science Center at San Antonio, San Antonio, TX

Abstract

T-cell protein tyrosine phosphatase (TC-PTP), encoded by *Ptpn2*, has been shown to function as a tumor suppressor during skin carcinogenesis. In the current study, we generated a novel epidermal specific TC-PTP-overexpressing (*K5HA.Ptpn2*) mouse model to show that TC-PTP contributes to the attenuation of chemically-induced skin carcinogenesis through the synergistic regulation of STAT1, STAT3, STAT5, and PI3K/AKT signaling. We found overexpression of TC-PTP increased epidermal sensitivity to DMBA-induced apoptosis and it decreased TPA-mediated hyperproliferation, coinciding with reduced epidermal thickness. Inhibition of STAT1, STAT3, STAT5 or AKT reversed the effects of TC-PTP overexpression on epidermal survival and proliferation. Mice overexpressing TC-PTP in the epidermis developed significantly reduced numbers of tumors during skin carcinogenesis and presented a prolonged latency of tumor initiation. Examination of human papillomas and squamous cell carcinomas (SCCs) revealed that TC-PTP expression was significantly reduced and TC-PTP expression was inversely correlated

[*]To whom correspondence should be addressed: Dae Joon Kim, 1214 W. Schunior St, Edinburg, TX 78541, dae.kim@utrgv.edu, Tel: 956-665-6411, Fax: 956-665-6402.

[#]These authors contributed equally to this work.

Author contributions

D.J.K. conceived the project, designed the study, and interpreted results. W.J.K., S.M., C.J., A.T., I.S.J., and T.J.S. also contributed to interpretation of results. C.J.L., L.D.M., M.K., S.A.O., and J.H. performed experiments. D.J.K. wrote the manuscript. All authors discussed the results and commented on the manuscript.

Conflict of Interest

No potential conflicts of interest were disclosed.

with the increased grade of SCCs. Our findings demonstrate that TC-PTP is a potential therapeutic target for the prevention of human skin cancer given that it is a major negative regulator of oncogenic signaling.

Keywords

TC-PTP; PTPN2; skin cancer; STAT; PI3K; AKT

Introduction

Phosphotyrosine-based signaling plays a significant role in maintaining cellular homeostasis. The posttranslational phosphorylation of proteins at tyrosine residues is catalyzed by protein tyrosine kinases, or PTKs, and the duration of the phosphorylation state is regulated by protein tyrosine phosphatases, or PTPs. Mutations that result in aberrant activation of PTKs can drive cell growth, proliferation, and survival. Therefore, a great deal of research has focused on understanding how to target dysregulated PTK signaling for anti-cancer therapies [1–3]. Studies utilizing loss-of-function mouse models further demonstrated that loss of PTP signaling is associated with various human diseases like cancer [4, 5]. However, the effect of PTP overexpression has not been sufficiently explored due to an initial failure to establish suitable PTP-overexpressing cell lines and models, especially in carcinogenesis [4, 6].

T-cell protein tyrosine phosphatase (TC-PTP) is an intracellular, non-receptor PTP encoded by the *PTPN2* gene [7, 8]. Alternative splicing at the 3’ end of *PTPN2* generates two distinct isoforms of TC-PTP: TC45 (45 kDa) and TC48 (48 kDa). TC45 is primarily found in the nucleus of most cell types, and shuttles between the nucleus and cytoplasm in response to growth factor and cytokine receptor signaling [9–11]. In keratinocytes, TC45 can be found in the cytoplasm, and it is shuttled to the nucleus by an AKT/14-3-3σ-mediated mechanism upon TC45 activation [12]. TC-PTP is involved in various cellular processes including cell proliferation, differentiation, and apoptosis through the negative regulation of its substrates, like JAK (janus kinase) 1, JAK3, STAT (signal transducer and activator of transcription) 1, and STAT3 [13–15]. Current research has shown that deletion or decreased expression of *PTPN2* occurs in human T-cell acute lymphoblastic leukemia, breast cancer and liver cancer [16–19]. Our studies demonstrated that TC-PTP functions *in vitro* and *in vivo* as a tumor suppressor in both UV- and chemically-induced skin cancer due to its ability to directly suppress STAT3 and Flk-1/VEGFR2 signaling [20, 21]. Together, these findings suggest that activation of TC-PTP would be an effective strategy against different types of cancer. However, an interesting recent study revealed that deletion of *PTPN2* in tumor cells increased their sensitivity to cancer immunotherapy [22]. Obviously, more research is needed to understand the full impact of PTP inhibition or activation on oncogenesis and the potential use of either in any anti-cancer strategies.

In the present study, we generated a new transgenic mouse model that overexpresses TC-PTP specifically in the epidermis (*K5HA.Ptpn2*) to further investigate the role of TC-PTP in chemically-induced skin carcinogenesis. TC-PTP overexpression significantly increased DMBA (7,12-dimethylbenz[a]anthracene)-induced epidermal apoptosis and reduced TPA

(12-*O*-tetradecanoylphorbol-13-acetate)-mediated epidermal hyperplasia and hyperproliferation through the regulation of STAT1, STAT3, STAT5, and PI3K (phosphatidylinositol-4,5-bisphosphate 3-kinase)/AKT signaling. Furthermore, *K5HA.Ptpn2* mice exposed to a DMBA/TPA regimen clearly exhibited delayed tumor development and significantly reduced tumor numbers compared to control mice. We also found TC-PTP expression was significantly lower in human papillomas and squamous cell carcinomas (SCCs) in comparison to normal skin tissue. Our findings provide additional evidence of the importance of TC-PTP in keratinocyte survival and proliferation and how its roles in these cellular mechanisms allow it to function as a major tumor suppressor in skin cancer.

Results

Generation of transgenic mice overexpressing TC-PTP in epidermis

In our previous study, we showed that TC-PTP that suppresses keratinocyte survival and proliferation in response to UVB exposure by directly dephosphorylating activated STAT3 [23]. Using a novel epidermal-specific TC-PTP knockout mouse model, we also demonstrated that TC-PTP has a critical role in attenuating chemically-induced skin cancer formation by regulating STAT3 and AKT phosphorylation [20]. To further investigate the functional role of TC-PTP in skin carcinogenesis, we generated transgenic mice that specifically overexpress TC-PTP in epidermis. HA-tagged mouse *Ptpn2* cDNA encoding TC-PTP [23] was amplified by PCR and cloned into the K5 expression vector containing rabbit β-globin intron and simian virus 40 polyadenylation signals to direct cDNA expression (Fig. 1a). The resulting transgene vector was injected into the pronuclei of donor embryos from FVB/N mice to generate TC-PTP-overexpressing mice under control of the K5 promoter (*K5HA.Ptpn2*). The FVB/N strain is highly sensitive to chemically-induced skin carcinogenesis in comparison to other strains, such as C57BL/N [24], and this strain also was used to generate our *Ptpn2* knockout mouse model. The transgenic mice were identified by PCR of the genomic DNA using primers specific for the rabbit β-globin intron. Three founders – identified as #2, #6, and #11 – were shown to carry the transgene by PCR analysis (Fig. 1b). Western blot analysis of epidermal lysates showed that of the three founders, #2 and #11 expressed exogenous TC-PTP as detected by anti-HA antibody and anti-TC-PTP antibody (Fig. 1c). In correlation with the overexpression of TC-PTP in epidermis, these two founders also exhibited decreased expression levels of phosphorylated STAT3 in comparison to non-transgenic (wild-type) littermates (Fig. 1c). Immunohistochemical analysis confirmed that TC-PTP transgenic mice expressed exogenous TC-PTP in the epidermis whereas control wild-type (WT) mice did not (Fig. 1d). Additionally, we analyzed protein lysates from other tissues harvested from TC-PTP transgenic mice and WT control and verified that exogenous TC-PTP was not expressed in these other tissues (Fig. 1e). Neither founder displayed any apparent physical differences from WT mice during maturation. Similarly, primary keratinocytes derived from both founders showed similar growth and morphological characteristics (Data not shown). Since the two founders exhibited similar molecular characteristics, growth patterns, and morphology, we utilized founder #11 for colony expansion and subsequent experiments.

Overexpression of TC-PTP increases susceptibility to DMBA-induced apoptosis

The tumor initiator DMBA causes DNA damage that can contribute to tumorigenesis if left unchecked; however, induction of the cell's natural apoptotic response can remove aberrant, damaged cells and prevents their proliferation [25, 26]. To investigate the effect of TC-PTP overexpression on apoptosis induced by DMBA, primary keratinocytes derived from either WT or *K5HA.Ptpn2* mice were cultured and treated with DMBA. There were no visible differences in morphology between control and TC-PTP-overexpressing keratinocytes before DMBA treatment (Fig. 2a). However, morphological changes characteristic of apoptosis, such as cell ballooning and bleb formation, were significantly increased in TC-PTP-overexpressing keratinocytes compared to control keratinocytes after DMBA treatment (Fig. 2a, b). Analysis of apoptosis utilizing flow cytometry demonstrated a clear increase of apoptotic cells in TC-PTP-overexpressing keratinocytes after DMBA treatment compared to control (Fig. 2c). We also compared primary keratinocytes derived from our TC-PTP-deficient mice [20] to control and TC-PTP-overexpressing keratinocytes after DMBA treatment. While the number of viable control or TC-PTP-overexpressing keratinocytes was decreased after treatment in comparison to untreated keratinocytes, the number of viable TC-PTP-deficient keratinocytes was not (Fig. 2d). Consistent with *in vitro* results, the number of apoptotic cells within the epidermis of *K5HA.Ptpn2* transgenic mice, which was detected by active caspase-3 staining, was significantly increased compared to control mice epidermis 24 h after DMBA treatment (Fig. 2e, f). These results support our hypothesis that TC-PTP plays a tumor suppressive role in epidermis by facilitating the removal of tumor-initiating keratinocytes upon DMBA exposure.

TC-PTP overexpression increases DMBA-induced apoptosis through the synergistic regulation of STAT1, STAT3, STAT5, and AKT signaling pathways

We have shown that TC-PTP dephosphorylates STAT3 in both mouse and human keratinocytes [23, 27]. We also have demonstrated that loss of TC-PTP promotes chemically-induced skin carcinogenesis through the activation of STAT3 and AKT signaling. To further investigate the role of TC-PTP in the regulation of these signaling pathways during DMBA-induced tumor initiation, primary keratinocytes derived from either WT or *K5HA.Ptpn2* mice were treated with different concentrations of DMBA for 1 h and then cultured in serum-free medium for 1 h in order to observe the initial response to DMBA. DMBA treatment increased the expression levels of tyrosine phosphorylated STAT3 (pY-STAT3) in control keratinocytes compared to TC-PTP-overexpressing keratinocytes; whereas serine phosphorylated STAT3 (pS-STAT3) was constitutively expressed in both genotypes in the presence or absence of DMBA (Fig. 3a). In our previous studies, we demonstrated that, unlike STAT3, neither STAT1 nor STAT5 were initially dephosphorylated by PTP in keratinocytes following UVB irradiation [27]. Similarly, DMBA did not induce either STAT1 or STAT5 activation in either genotype during the 1 h culture period following treatment (Fig. 3a). Additionally, we examined the effects of TC-PTP overexpression on PI3K/AKT signaling during the cellular response to DMBA, and we found phosphorylation of PI3K, the upstream regulator of AKT, was completely blocked by DMBA treatment in both genotypes. The expression levels of phosphorylated AKT in control keratinocytes was higher in comparison to TC-PTP-overexpressing keratinocytes after DMBA treatment (Fig. 3b).

Next, primary keratinocytes derived from both genotypes were treated with DMBA for 1 h and then cultured over a 24 h period to evaluate the effect of TC-PTP overexpression on the long-term response to DMBA. Western blot analysis showed that DMBA treatment induced an increase in the expression levels of pY-STAT3 and phosphorylated AKT in control keratinocytes when compared to TC-PTP-overexpressing keratinocytes. We also observed that the levels of pY-STAT5 were increased in control keratinocytes when compared to TC-PTP-overexpressing keratinocytes during the long-term (24 h) culture period following DMBA treatment (Fig. 3c). Furthermore, while the expression levels of pY-STAT1 and total STAT1 were higher in control keratinocytes in comparison to *K5HA.Ptpn2* keratinocytes following DMBA treatment, the levels of pS-STAT1 were increased in *K5HA.Ptpn2* keratinocytes compared to control (Fig. 3c). The expression levels of Bax and cleaved caspase 3 also were higher in *K5HA.Ptpn2* keratinocytes (Fig. 3c), suggesting serine phosphorylation of STAT1 corresponds to increased DMBA-induced apoptosis.

Inhibition of STAT3, STAT5 or AKT with a specific inhibitor before DMBA treatment significantly reduced cell viability in WT cells in comparison to DMBA-only control cells (Fig. 4a–c). On the other hand, STAT1 inhibition significantly increased cell viability in TC-PTP-overexpressing keratinocytes in comparison to DMBA-only control cells (Fig. 4a, d), indicating that tyrosine phosphorylation of STAT1 does not play a role in the cell viability of keratinocytes during tumor initiation. Our findings suggest that TC-PTP protects keratinocytes during tumor initiation by promoting DMBA-induced apoptosis via the positive regulation of STAT1 serine phosphorylation and the negative regulation of STAT3, STAT5, and AKT signaling.

TC-PTP overexpression suppresses TPA-induced epidermal hyperproliferation and hyperplasia

DNA-damaged cells that escape apoptosis during tumor initiation possess a growth advantage that drives proliferation, resulting in epidermal hyperplasia during tumor promotion [26]. To examine whether TC-PTP overexpression can reduce TPA-induced keratinocyte hyperproliferation and epidermal hyperplasia, primary keratinocytes derived from WT and *K5HA.Ptpn2* mice were cultured. TC-PTP-overexpressing keratinocytes grew significantly slower than control keratinocytes after 48 and 72 h of culture (Fig. 5a). Keratinocytes from both genotypes showed an initial decrease in growth rate after TPA treatment for 1 h. Following the short lag period, both cell lines began to grow again. However, TC-PTP-overexpressing keratinocytes proliferated significantly slower than WT (Fig. 5b, c).

To examine whether or not overexpression of TC-PTP has an inhibitory effect on TPA-induced hyperproliferation and hyperplasia *in vivo*, both control and TC-PTP transgenic mice were treated with TPA over a 72 h period. As shown in Fig. 4d and e, there were no significant differences in the epidermal thickness between the two genotypes in the absence of treatment. However, topical application of TPA significantly increased epidermal thickness of WT mice in comparison to *K5HA.Ptpn2* transgenic mice 24, 48, and 72 h after treatment (Fig. 5d, e). Analysis of epidermal cell proliferation using BrdU labeling and PCNA staining also showed similar results. Following TPA treatment, the number of either

BrdU-positive or PCNA-positive cells in the epidermis of WT mice was significantly increased compared to *K5HA.Ptpn2* transgenic mice (Fig. 5f–i). These findings further demonstrate that TC-PTP can protect skin against TPA-induced epidermal hyperproliferation and hyperplasia.

TC-PTP overexpression reduces TPA-induced proliferation through the synergistic regulation of STAT1, STAT3, STAT5, and PI3K/AKT signaling pathways

To investigate the regulatory role of TC-PTP during tumor promotion, primary keratinocytes from both WT and *K5HA.Ptpn2* mice were treated with TPA for 1 h and then cultured over a four hour period in order to observe the initial response to TPA. As shown in Fig. 6a, TPA treatment induced a significant increase of pY-STAT3, pY-STAT1 and pY-STAT5 expression levels over time in control keratinocytes in comparison to TC-PTP-overexpressing keratinocytes. In contrast, TC-PTP-overexpressing keratinocytes showed a significant increase of pS-STAT1 in response to TPA treatment (Fig. 6a). Overexpression of TC-PTP also inhibited phosphorylation of PI3K in the presence and absence of TPA. Consistently, the levels of phosphorylated AKT in control were higher when compared to TC-PTP-overexpressing keratinocytes with or without TPA treatment (Fig. 6b).

Next, primary keratinocytes from both genotypes were treated with TPA for 1 h and then cultured over a 72 h period to check the long term effect of TC-PTP overexpression on the response to TPA treatment. Western blot analysis revealed a decrease of pY-STAT3 over time in both genotypes; but, levels of pY-STAT3 in TC-PTP-overexpressing keratinocytes were, again, clearly reduced in comparison to wild-type (Fig. 6c). There was little to no expression of pY-STAT1 or pY-STAT5 in either keratinocyte genotype. However, the results revealed an increase of pS-STAT1 24 h after TPA treatment in both genotypes, with *K5HA.Ptpn2* keratinocytes expressing higher levels of pS-STAT1 than wild-type keratinocytes even though the level of total STAT1 was lower in TC-PTP-overexpressing cells than control cells (Fig. 6c). Like STAT3, TPA treatment reduced phosphorylation of PI3K over time; however, levels of phosphorylated PI3K were much lower in TC-PTP-overexpressing keratinocytes than control keratinocytes (Fig. 6c). Consequently, the level of phosphorylated AKT was lower in TC-PTP-overexpressing cells than control cells following TPA exposure. To examine the potential effects of STAT- and PI3K/AKT-mediated signaling on cell proliferation and apoptosis, we analyzed the expression levels of different well-known markers. Expression of cyclin D1 appeared to be higher in WT keratinocytes compared to TC-PTP-overexpressing keratinocytes (Fig. 6c). The levels of the anti-apoptotic proteins Bcl-2 and Bcl-xL were also higher in WT cells than TC-PTP-overexpressing cells and they showed a time-dependent increase. In contrast, expression levels of Bax increased in a time-dependent manner only in *K5HA.Ptpn2* keratinocytes (Fig. 6c).

Inhibition of either STAT3 or STAT5 with a specific inhibitor prior to TPA treatment significantly reduced cell viability in WT cells compared to TC-PTP-overexpressing cells (Fig. 7a, b). However, inhibition of both STAT3 and STAT5 did not further reduce cell viability in WT (Fig. 7b), suggesting STAT3 and STAT5 regulate the same or similar downstream targets/signaling pathways during TPA-induced keratinocyte proliferation. Previous studies showed that TPA induced STAT1 tyrosine phosphorylation in mouse

epidermis; yet, STAT1 did not have an effect on TPA-induced skin tumor promotion and formation [28]. We found inhibition of STAT1 prior to TPA treatment did not reduce cell viability in WT keratinocytes. In contrast, STAT1 inhibition significantly increased cell viability in TC-PTP-overexpressing keratinocytes, implying that TC-PTP-mediated serine phosphorylation of STAT1 inhibits TPA-induced cell proliferation (Fig. 7c). Analysis of the cell cycle by flow cytometry confirmed that TC-PTP-overexpressing cells treated with STAT1 inhibitor before TPA exposure showed an increase of cells in the S phase and the G2/M phase of the cell cycle (Fig. 7d; Supplementary Fig. S1). Similar results were observed for PI3K/AKT signaling. Inhibition of either PI3K or AKT prior to addition of TPA significantly reduced cell viability in control keratinocytes; however, their inhibition had no effect on cell viability of TC-PTP-overexpressing keratinocytes (Fig. 7e, f). These findings suggest that TC-PTP protects keratinocytes during tumor promotion by inhibiting TPA-induced cell proliferation via the negative regulation of STAT3, STAT5, and PI3K/AKT signaling, and the positive regulation of STAT1 signaling.

Overexpression of TC-PTP reduces prevalence of skin tumors stimulated by DMBA/TPA regimen in mouse

To examine the role of TC-PTP in TPA-induced hyperproliferation and hyperplasia *in vivo*, both control and TC-PTP transgenic mice were treated with TPA twice weekly for two weeks. As shown in Fig. 8a and b, repeated application of TPA to the epidermis significantly increased epidermal thickness of WT mice in comparison to *K5HA.Ptpn2* transgenic mice 24 and 48 h after last treatment. Then, TC-PTP transgenic and WT mice were subjected to a two-stage chemical carcinogenesis regimen. Both groups of mice were treated with DMBA. Two weeks after tumor initiation with DMBA, mice were treated with TPA twice weekly to promote tumor formation. Mice overexpressing TC-PTP in skin were less susceptible to chemically-induced skin carcinogenesis in comparison to control (Fig. 8c–e). WT mice started to develop papilllomas 8 weeks after promotion, whereas transgenic mice did not develop papillomas until 10 weeks after promotion (Fig. 8d). By 15 weeks, 100% of the control group had developed papillomas while only ~80% of the transgenic group had developed papillomas (Fig. 8d). This difference was statistically significant after 8 weeks and for the remainder of the experiment ($P < 0.05$, Likelihood Ratio test). The average number of papillomas per mouse was greater in WT compared with *K5HA.Ptpn2* mice (Fig. 8e). There was a significant reduction in the average number of papillomas per mouse in *K5HA.Ptpn2* transgenic mice compared to WT mice after 10 weeks and for the remainder of the experiment ($P < 0.05$ by Mann-Whitney U test, Fig. 8e). Immunohistochemical analysis confirmed that papillomas from *K5HA.Ptpn2* mice expressed both exogenous HA-tagged TC-PTP and endogenous TC-PTP, whereas papillomas from WT mice did not (Fig. 8f). Furthermore, papillomas from TC-PTP overexpressing mice showed a clear decrease in levels of phosphorylated STAT3 and phosphorylated AKT expression in comparison to control (Fig. 8f).

TC-PTP expression is reduced in human skin tumors

We also analyzed the expression of TC-PTP in human skin tumors in order to demonstrate the potential significance of our findings in mice. Immunohistochemical analysis showed that TC-PTP was expressed in normal human skin sections (n=13), but its expression was

significantly decreased in both papillomas (n=6) and squamous cell carcinomas (SCCs) (n=57) (Fig. 9a, b). TC-PTP expression was further decreased with increased grade of human SCCs (Fig. 9c, d). Immunohistochemical staining of phosphorylated STAT3 (p-STAT3) and phosphorylated AKT (p-AKT) revealed that their expression levels were higher in papillomas and SCCs compared to normal skin sections (Fig. 9e), Quantification of staining revealed expression of p-STAT3 was significantly ($P < 0.0001$) inversely correlated with TC-PTP expression, and p-AKT expression appeared to decrease ($P = 0.044$) with increased TC-PTP expression. (Fig. 9f, g). These findings imply that loss of TC-PTP-mediated regulation of STAT3 and AKT signaling may play an important role in human skin tumor progression.

Discussion

Many studies have demonstrated that PTPs are involved in the regulation of carcinogenesis, either as tumor suppressors or tumor promoters. Our early studies showed that PTPs are initially activated in response to UVB irradiation to protect keratinocytes from DNA damage-induced transformation through the negative regulation of STAT3 survival signaling [27]. Further investigation revealed that TC-PTP is the key PTP involved in the regulation of STAT3 signaling in keratinocytes following UVB exposure [23]. Recent studies using an epidermal specific TC-PTP knockout mouse model demonstrated that TC-PTP deficiency promotes resistance to apoptosis and hyperproliferation in the epidermis by regulating both STAT3 and AKT signaling pathways. Moreover, TC-PTP deficiency in epidermis significantly accelerated skin tumor formation in mouse during skin carcinogenesis induced by DMBA/TPA [20]. In the current study, we further demonstrate that TC-PTP is a critical tumor suppressor in skin cancer development by generating and characterizing an epidermal-specific TC-PTP overexpressing mouse model.

Previous studies showed that three STATs – STAT1, STAT3, and STAT5 – are activated in the epidermis after TPA treatment [29]. We found all three STATs were phosphorylated at a tyrosine residue in wild-type primary keratinocytes after either DMBA or TPA treatment, but, TC-PTP overexpression blocked tyrosine phosphorylation (Fig. 3c, 6a). Our previous studies showed that TPA treatment initially reduced the level of pY-STAT3 in control keratinocytes compared to TC-PTP-deficient keratinocytes [20]. The current results demonstrated the level of pY-STAT3 expression quickly recovered (at 1 h) post TPA treatment and gradually increased with time, however overexpression of TC-PTP completely inhibited STAT3 phosphorylation (Fig. 6a). Additionally, we had previously found that while the expression levels of pY-STAT3 were initially decreased in keratinocytes after UVB exposure, the levels of pY-STAT1 and pY-STAT5 remained changed [27]. On the other hand, our current results indicated that DMBA or TPA can induce tyrosine phosphorylation of the three STATs, and their tyrosine phosphorylation was negatively regulated by TC-PTP. Interestingly, whereas wild-type primary keratinocytes expressed higher levels of pY-STAT1 than TC-PTP-overexpressing primary keratinocytes, the levels of pS-STAT1 were increased in TC-PTP-overexpressing keratinocytes compared to control keratinocytes after either DMBA or TPA treatment (Fig. 3c, 6a). Serine phosphorylation of STAT1 is known to be crucial for maximal transcriptional activation and STAT1 interaction with transcriptional co-factors [30–32]. Studies have shown that serine phosphorylation of STAT1 promotes

apoptosis. It is required for oxysterol-induced apoptosis given that it induces $p21^{waf1}$ expression [33]. It also has been demonstrated that PKCδ–dependent phosphorylation of STAT1 at serine residue increases apoptosis [34]. Similar with these findings, our results showed inhibition of serine phosphorylation of STAT1 in TC-PTP-overexpressing cells significantly increased cell survival after either DMBA or TPA treatment (Fig. 4d and 7c). It was noted that even though the levels of pS-STAT1 were higher in TC-PTP-overexpressing cells than control cells, the level of unphosphorylated STAT1 was lower in TC-PTP-overexpressing cells than control cells in the absence or presence of TPA treatment (Fig. 6a, c). Studies have demonstrated that unphosphorylated STAT1 can promote tumor development by repressing apoptosis [35]. It is possible that TC-PTP-mediated downregulation of STAT1 expression may contribute to increased apoptosis and decreased cell growth in keratinocytes.

PI3K signaling is one of the major cell survival and proliferation signaling pathways that contribute to cancer development given that it is an upstream kinase of AKT [36, 37]. Both wild-type and TC-PTP-overexpressing keratinocytes cultured in serum-free medium constitutively expressed pY-PI3K but its expression was inhibited in both genotypes after DMBA treatment (Fig. 3b). However, AKT was still activated in response to DMBA, suggesting that PI3K-independent activation of AKT contributes to the inhibition of DMBA-induced apoptosis. In normal keratinocyte medium, pY-PI3K was constitutively expressed in wild-type cells only and its expression levels remained the same until 4 h after TPA treatment. Again, PI3K activation was completely inhibited in TC-PTP-overexpressing cells (Fig. 6b). We found that TC-PTP did not directly dephosphorylate pY-PI3K (Supplementary Fig. S2). While the interaction of TC-PTP with STAT3 was increased following TPA treatment, TC-PTP didn’t interact with PI3K in the presence or absence of TPA in keratinocytes. Therefore, further studies remain to be done to elucidate the mechanism by which TC-PTP overexpression prevents PI3K phosphorylation. In addition, it is possible that TC-PTP can also regulate DMBA metabolism or DNA damage or repair after DMBA treatment by dephosphorylating unknown substrates involved in this mechanism, which can increase epidermal apoptosis. Further studies are needed to investigate the detailed mechanism by which TC-PTP regulates DMBA-induced apoptosis.

Chemical carcinogenesis studies using *K5HA.Ptpn2* mice confirmed a tumor suppressive role for TC-PTP in skin cancer development (Fig. 8c–e). Overexpression of TC-PTP suppressed skin cancer formation as evidenced by the overall reduction in tumor incidence and numbers of tumors. Additionally, we found TC-PTP expression was significantly decreased in human skin papillomas and SCCs and further decreased with increased grade of SCCs (Fig. 9a–d). Generation of transgenic mice that express a constitutively active form of TC-PTP or utilization of a TC-PTP activator may be useful methods to further understand the tumor suppressive role of TC-PTP in skin carcinogenesis. In summary, our investigation provided evidence that TC-PTP may be a potential marker for prognosis and modulation of TC-PTP expression/activation may be a new therapeutic approach in the prevention and treatment of skin cancer.

Materials and Methods

Generation of epidermal-specific TC-PTP-overexpressing (*K5HA.Ptpn2*) mice.

Transgenic mice that overexpress *Ptpn2* in the epidermis were generated by microinjection of a bovine keratin 5 (K5) targeting vector containing HA-tagged *Ptpn2* into the pronuclei of donor embryos to produce transgenic founders on FVB/N genetic background. Briefly, HA-tagged full-length mouse *Ptpn2* cDNA from pCMV6/AN/HA [23] was amplified by PCR and cloned into the NheI and SnaBI sites of the K5 targeting vector. The resulting transgene vector was digested with KpnI, purified using Qiagen DNA gel extraction kit and injected into the pronuclei. Transgenic mice were identified by PCR of genomic DNA isolated from tail snips using oligonucleotides specific for the gene encoding rabbit β-globin intron; 5'-TTC AGG GTG TTG TTT AGA ATG G-3' and 5'-CAA TAA GAA TAT TTC CAC GCC A-3'. All experiments were performed using 6–8 weeks old female mice, unless otherwise indicated. The dorsal skin of each mouse was shaved 48 h before treatment; only those mice in the resting phase of hair cycle were used. All experiments with mice were carried out with strict adherence to both institutional and National Institutes of Health (NIH) guidelines for minimizing distress in experimental animals, and animal usage was approved by the University of Texas Rio Grande Valley, Institutional Animal Care and Use Committee.

Primary keratinocyte cell culture.

Two day-old non-transgenic or *K5HA.Ptpn2* neonates were used to culture primary keratinocytes as described previously [38]. Briefly, neonates were euthanized and skin was surgically removed. The skin was then placed in trypsin for 12 h at 4 °C to remove the dermis. Then, the isolated epidermis was minced and filtered through a cell strainer (70 μm) to remove debris. Primary keratinocytes were plated and cultured at 37 °C and 5% CO_2 in low Ca^{2+} (0.03 mM) KGM-2 medium (Lonza, #CC-3158) containing 1% penicillin/streptomycin and 1% fetal bovine serum until 60 to 70% confluency at which time cells were treated with DMBA or TPA.

Flow cytometric analysis.

Apoptosis of primary keratinocytes was evaluated using Annexin V-FITC apoptosis kit (Molecular probe, V13242) according of the manufacturer's instructions. Briefly, cells were harvested with 0.25% trypsin; 1×10^6 cells were then washed with cold PBS and centrifuged at 350 × g for 10 min and stained using Annexin V-FITC. Then, cell suspensions were analyzed using LSRFortessa (BD Biosciences). The apoptotic rate was calculated as of Annexin V-positive cells. Each experiment was performed three times, and data were presented as the means ± SD. The cell cycle was analyzed using FXCycle™ Violet Ready Flow™ Reagent (Invitrogen, R37166) according to the manufacturer's instructions. Briefly, Primary keratinocytes obtained from wild-type and *K5HA.Ptpn2* neonates were incubated in serum-free medium the day before treatment with TPA or TPA and STAT1 inhibitor Fludarabine (10 μM). Twelve hours after treatment, cells were harvested with 0.25% trypsin; 1×10^6 cells were then washed with cold PBS and centrifuged at 350 × g for 5 min and stained using FXCycle. Then, cell suspensions were analyzed using LSRFortessa. Each experiment was performed three times, and data were presented as the means ± SD.

Two-stage carcinogenesis.

Female wild-type and *K5HA.Ptpn2* littermates at 7–8 weeks of age (n=13/group) were initiated with 25 nmol of DMBA. Two weeks after DMBA treatment, mice received topical treatments of 6.8 nmol TPA twice a week until the experiment was terminated. Tumor incidence (percentage of mice with papillomas) and tumor multiplicity (average number of papillomas per mouse) were determined weekly until multiplicity plateaued. Differences in tumor incidence and multiplicity were analyzed by the Likelihood Ratio test and the Mann-Whitney U test, respectively.

Immunohistochemical analysis.

The dorsal skin of mouse was fixed in 10% neutral-buffered formalin after sacrifice. Human skin cancer and normal tissues were purchased from Reveal Biosciences (#SK04), BioChain® (#T2235218–7&8), and SUPER BIO CHIPS (#CX2). Formalin-fixed and paraffin-embedded tissues were deparaffinized and hydrated using standard procedures. Endogenous peroxidase activity was blocked with 0.03% hydrogen peroxide for 10 min. For the antigen retrieval, sections were microwaved for 5 min in 10 mM sodium citrate buffer (pH 6.0) containing 0.01% Tween 20 and allowed to cool for 20 min. Sections were then stained with anti-TC-PTP (Proteintech, #11214–1-AP), anti-p-STAT3 (Tyr705) (#9145) and anti-p-AKT (Thr308) (#13038) (Cell Signaling Technology) antibodies following suggested procedures by the manufacturer. All specimens were assessed by H&E staining for morphology. Immunoreactivity was determined by scoring according to the staining intensity (0, none; 1, weak; 2, moderate; 3, strong) of immunolabeling and percent positive cells (0, <5%; 1, 6 to 25%; 2, 26 to 50%; 3, 51 to 75%; 4, 76% to 100%). The final immunoreactive score was calculated by multiplying positive cells proportion score by staining intensity score. In the above analysis, there was no discrepancy between the 2 observers regarding the patterns of biomarker expression and the scores assigned to analyzed sections. Data were quantified and analyzed with Image J software.

Supplementary Material

Refer to Web version on PubMed Central for supplementary material.

Acknowledgments

We thank H Lee for technical assistance. This work was supported by NIH/NIEHS ES022250 (to D.J. Kim) and NIH/NIAID AI119131 (to S.Mummidi).

References

1. Lim WA, Pawson T. Phosphotyrosine signaling: evolving a new cellular communication system. Cell 2010; 142: 661–667. [PubMed: 20813250]
2. Hunter T. Tyrosine phosphorylation: thirty years and counting. Curr Opin Cell Biol 2009; 21: 140–146. [PubMed: 19269802]
3. Casaletto JB, McClatchey AI. Spatial regulation of receptor tyrosine kinases in development and cancer. Nat Rev Cancer 2012; 12: 387–400. [PubMed: 22622641]
4. Hendriks WJ, Elson A, Harroch S, Stoker AW. Protein tyrosine phosphatases: functional inferences from mouse models and human diseases. FEBS J 2008; 275: 816–830. [PubMed: 18298790]

5. Hendriks WJ, Pulido R. Protein tyrosine phosphatase variants in human hereditary disorders and disease susceptibilities. Biochim Biophys Acta 2013; 1832: 1673–1696. [PubMed: 23707412]
6. Cuppen E, Wijers M, Schepens J, Fransen J, Wieringa B, Hendriks W. A FERM domain governs apical confinement of PTP-BL in epithelial cells. J Cell Sci 1999; 112 (Pt 19): 3299–3308. [PubMed: 10504335]
7. Cool DE, Tonks NK, Charbonneau H, Walsh KA, Fischer EH, Krebs EG. cDNA isolated from a human T-cell library encodes a member of the protein-tyrosine-phosphatase family. Proc Natl Acad Sci U S A 1989; 86: 5257–5261. [PubMed: 2546150]
8. Mosinger B Jr., Tillmann U, Westphal H, Tremblay ML. Cloning and characterization of a mouse cDNA encoding a cytoplasmic protein-tyrosine-phosphatase. Proc Natl Acad Sci U S A 1992; 89: 499–503. [PubMed: 1731319]
9. Bourdeau A, Dube N, Tremblay ML. Cytoplasmic protein tyrosine phosphatases, regulation and function: the roles of PTP1B and TC-PTP. Curr Opin Cell Biol 2005; 17: 203–209. [PubMed: 15780598]
10. Tillmann U, Wagner J, Boerboom D, Westphal H, Tremblay ML. Nuclear localization and cell cycle regulation of a murine protein tyrosine phosphatase. Mol Cell Biol 1994; 14: 3030–3040. [PubMed: 8164659]
11. Kamatkar S, Radha V, Nambirajan S, Reddy RS, Swarup G. Two splice variants of a tyrosine phosphatase differ in substrate specificity, DNA binding, and subcellular location. J Biol Chem 1996; 271: 26755–26761. [PubMed: 8900155]
12. Kim M, Morales LD, Baek M, Slaga TJ, DiGiovanni J, Kim DJ. UVB-induced nuclear translocation of TC-PTP by AKT/14-3-3sigma axis inhibits keratinocyte survival and proliferation. Oncotarget 2017; 8: 90674–90692. [PubMed: 29207596]
13. Dube N, Tremblay ML. Involvement of the small protein tyrosine phosphatases TC-PTP and PTP1B in signal transduction and diseases: from diabetes, obesity to cell cycle, and cancer. Biochim Biophys Acta 2005; 1754: 108–117. [PubMed: 16198645]
14. Xu D, Qu CK. Protein tyrosine phosphatases in the JAK/STAT pathway. Front Biosci 2008; 13: 4925–4932. [PubMed: 18508557]
15. Kim M, Morales LD, Jang IS, Cho YY, Kim DJ. Protein Tyrosine Phosphatases as Potential Regulators of STAT3 Signaling. Int J Mol Sci 2018; 19.
16. Shields BJ, Wiede F, Gurzov EN, Wee K, Hauser C, Zhu HJ et al. TCPTP regulates SFK and STAT3 signaling and is lost in triple-negative breast cancers. Mole Cell Biol 2013; 33: 557–570.
17. Kleppe M, Lahortiga I, El Chaar T, De Keersmaecker K, Mentens N, Graux C et al. Deletion of the protein tyrosine phosphatase gene PTPN2 in T-cell acute lymphoblastic leukemia. Nat Genet 2010; 42: 530–535. [PubMed: 20473312]
18. Lee CF, Ling ZQ, Zhao T, Fang SH, Chang WC, Lee SC et al. Genomic-wide analysis of lymphatic metastasis-associated genes in human hepatocellular carcinoma. World J Gastroenterol 2009; 15: 356–365. [PubMed: 19140237]
19. Karlsson E, Veenstra C, Emin S, Dutta C, Perez-Tenorio G, Nordenskjold B et al. Loss of protein tyrosine phosphatase, non-receptor type 2 is associated with activation of AKT and tamoxifen resistance in breast cancer. Breast Cancer Res Treat 2015; 153: 31–40. [PubMed: 26208487]
20. Lee H, Kim M, Baek M, Morales LD, Jang IS, Slaga TJ et al. Targeted disruption of TC-PTP in the proliferative compartment augments STAT3 and AKT signaling and skin tumor development. Sci Rep 2017; 7: 45077. [PubMed: 28322331]
21. Baek M, Kim M, Lim JS, Morales LD, Hernandez J, Mummidi S et al. Epidermal-specific deletion of TC-PTP promotes UVB-induced epidermal cell survival through the regulation of Flk-1/JNK signaling. Cell Death Dis 2018; 9: 730. [PubMed: 29955047]
22. Manguso RT, Pope HW, Zimmer MD, Brown FD, Yates KB, Miller BC et al. In vivo CRISPR screening identifies Ptpn2 as a cancer immunotherapy target. Nature 2017; 547: 413–418. [PubMed: 28723893]
23. Lee H, Morales LD, Slaga TJ, Kim DJ. Activation of T-cell protein-tyrosine phosphatase suppresses keratinocyte survival and proliferation following UVB irradiation. J Biol Chem 2015; 290: 13–24. [PubMed: 25406309]

24. Hennings H, Glick AB, Lowry DT, Krsmanovic LS, Sly LM, Yuspa SH. FVB/N mice: an inbred strain sensitive to the chemical induction of squamous cell carcinomas in the skin. Carcinogenesis 1993; 14: 2353–2358. [PubMed: 8242866]
25. Abel EL, Angel JM, Kiguchi K, DiGiovanni J. Multi-stage chemical carcinogenesis in mouse skin: fundamentals and applications. Nat Protoc 2009; 4: 1350–1362. [PubMed: 19713956]
26. DiGiovanni J. Multistage carcinogenesis in mouse skin. Pharmacol Ther 1992; 54: 63–128. [PubMed: 1528955]
27. Kim DJ, Tremblay ML, Digiovanni J. Protein tyrosine phosphatases, TC-PTP, SHP1, and SHP2, cooperate in rapid dephosphorylation of Stat3 in keratinocytes following UVB irradiation. PLoS One 2010; 5: e10290. [PubMed: 20421975]
28. Bozeman R, Abel EL, Macias E, Cheng T, Beltran L, DiGiovanni J. A novel mechanism of skin tumor promotion involving interferon-gamma (IFNgamma)/signal transducer and activator of transcription-1 (Stat1) signaling. Mol Carcinog 2015; 54: 642–653. [PubMed: 24464587]
29. Chan KS, Carbajal S, Kiguchi K, Clifford J, Sano S, DiGiovanni J. Epidermal growth factor receptor-mediated activation of Stat3 during multistage skin carcinogenesis. Cancer Res 2004; 64: 2382–2389. [PubMed: 15059889]
30. Kumar A, Commane M, Flickinger TW, Horvath CM, Stark GR. Defective TNF-alpha-induced apoptosis in STAT1-null cells due to low constitutive levels of caspases. Science 1997; 278: 1630–1632. [PubMed: 9374464]
31. Zhang JJ, Zhao Y, Chait BT, Lathem WW, Ritzi M, Knippers R et al. Ser727-dependent recruitment of MCM5 by Stat1alpha in IFN-gamma-induced transcriptional activation. EMBO J 1998; 17: 6963–6971. [PubMed: 9843502]
32. Wen Z, Zhong Z, Darnell JE, Jr. Maximal activation of transcription by Stat1 and Stat3 requires both tyrosine and serine phosphorylation. Cell 1995; 82: 241–250. [PubMed: 7543024]
33. Agrawal S, Agarwal ML, Chatterjee-Kishore M, Stark GR, Chisolm GM. Stat1-dependent, p53-independent expression of p21(waf1) modulates oxysterol-induced apoptosis. Mol Cell Biol 2002; 22: 1981–1992. [PubMed: 11884587]
34. DeVries TA, Kalkofen RL, Matassa AA, Reyland ME. Protein kinase Cdelta regulates apoptosis via activation of STAT1. J Biol Chem 2004; 279: 45603–45612. [PubMed: 15322115]
35. Zimmerman MA, Rahman NT, Yang D, Lahat G, Lazar AJ, Pollock RE et al. Unphosphorylated STAT1 promotes sarcoma development through repressing expression of Fas and bad and conferring apoptotic resistance. Cancer Res 2012; 72: 4724–4732. [PubMed: 22805310]
36. Liu P, Cheng H, Roberts TM, Zhao JJ. Targeting the phosphoinositide 3-kinase pathway in cancer. Nat Rev Drug Discov 2009; 8: 627–644. [PubMed: 19644473]
37. Martini M, De Santis MC, Braccini L, Gulluni F, Hirsch E. PI3K/AKT signaling pathway and cancer: an updated review. Ann Med 2014; 46: 372–383. [PubMed: 24897931]
38. Dlugosz AA, Glick AB, Tennenbaum T, Weinberg WC, Yuspa SH. Isolation and utilization of epidermal keratinocytes for oncogene research. Methods Enzymol 1995; 254: 3–20. [PubMed: 8531694]

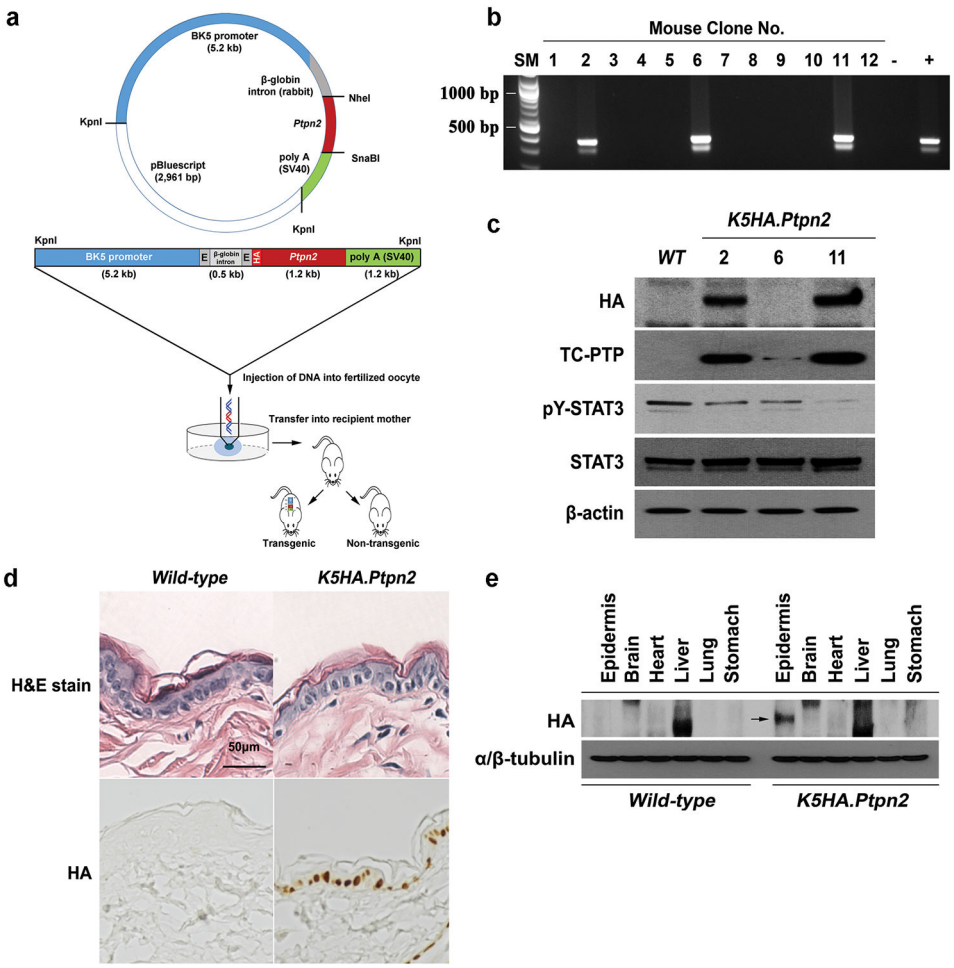

Figure 1. Generation of epidermal-specific *K5HA.Ptpn2* transgenic mouse.

a Schematic diagram of the construct used to generate HA-tagged TC-PTP (*Ptpn2*) transgenic mice using the BK5 promoter. **b** Genomic PCR analysis of the transgene using genomic DNA obtained from the mouse tail. PCR was performed using the two primers described in Materials and Methods to identify the transgenic founders. **c** Western blot analysis of HA, TC-PTP, p-STAT3 and STAT3 in the epidermis from non-transgenic wild-type (WT) and *K5HA.Ptpn2* mice. Epidermis was collected and total cell lysates from both genotypes were resolved by SDS-PAGE and immunoblotted with antibodies specific for HA, TC-PTP, p-STAT3 and STAT3. **d** Representative hematoxylin & eosin (H&E) staining and immunohistochemical staining of HA-tagged TC-PTP using HA antibody in the epidermis from both genotypes. Scale bar: 50 μm. **e** Western blot analysis of HA in non-epidermal tissues from wild-type and *K5HA.Ptpn2* mice. Brain, heart, liver, lung, and stomach were collected from both genotypes and total cell lysates were prepared.

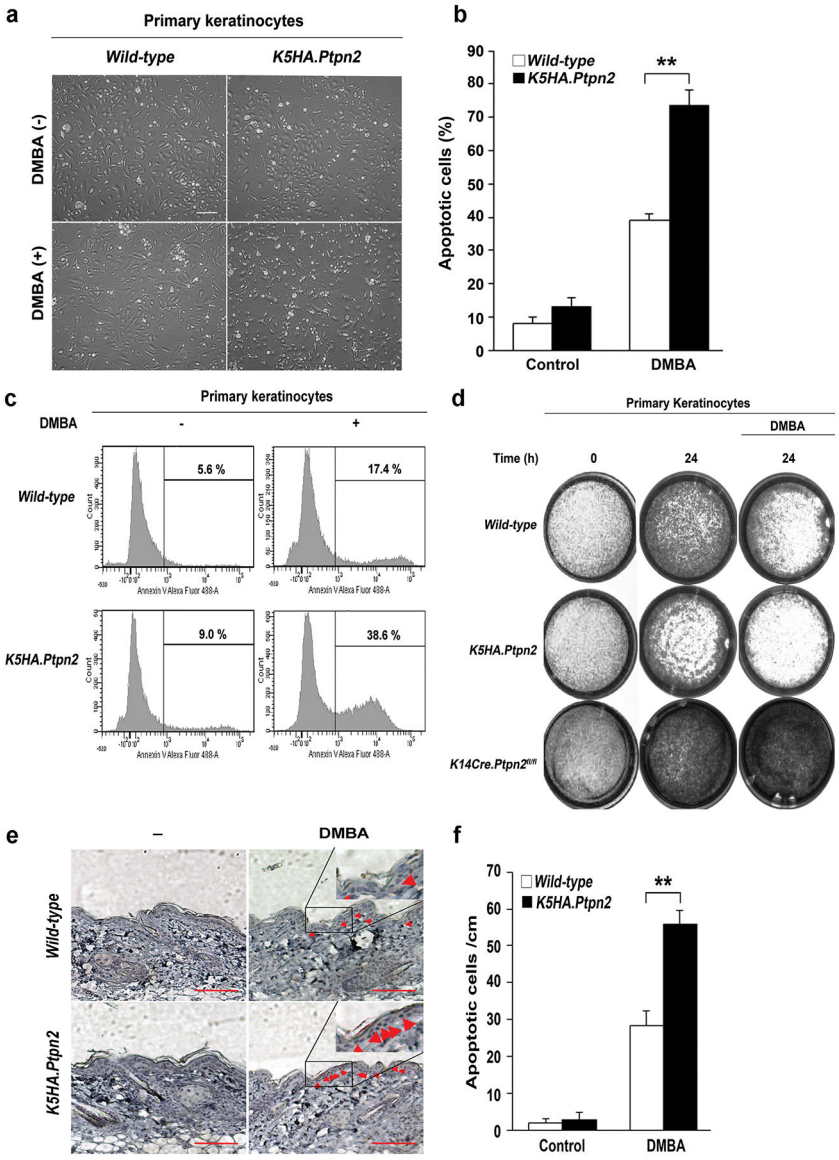

Figure 2. Effect of TC-PTP overexpression on DMBA-induced apoptosis in epidermis.

a-d Apoptotic response of primary keratinocytes obtained from the epidermis of wild-type and *K5HA.Ptpn2* mice after 24 h of DMBA treatment. **a** Primary keratinocytes from both genotypes were cultured and treated with 50 nM of DMBA. Scale bar: 100 μm. **b** Quantitative analysis of percentage of apoptotic cells characterized by cell ballooning, nuclear condensation, and bleb formation. After 24 h of DMBA treatment, apoptotic keratinocytes were counted microscopically in at least three non-overlapping fields. Results are the mean ± s.d.m. from three independent experiments. **, $P < 0.01$ by Mann-Whitney *U* test. **c** Quantification of apoptotic cells in primary keratinocytes from both genotypes 24 h after DMBA treatment. Apoptotic cells were stained with Annexin V-FITC and analyzed by using flow cytometry. **d** Representative crystal violet staining of primary keratinocytes from wild-type, *K5HA.Ptpn2*, *K14Cre.Ptpn2*$^{fl/fl}$ mice following 24 h of DMBA treatment. **e-f** Apoptotic response of the epidermis from both genotypes. Groups of mice (n=3) were

received a single topical application of DMBA (200 nmol) and sacrificed 24 h later. Skin sections were collected and apoptotic cells were quantified by immunostaining with caspase-3. **e** Representative staining of caspase-3 in the epidermis from both genotypes following treatment with DMBA. Scale bar: 100 μm. **f** Quantitative analysis of caspase-3-positive cells per centimeter of epidermis in both genotypes after DMBA treatment. **, $P < 0.01$ by Mann-Whitney U test.

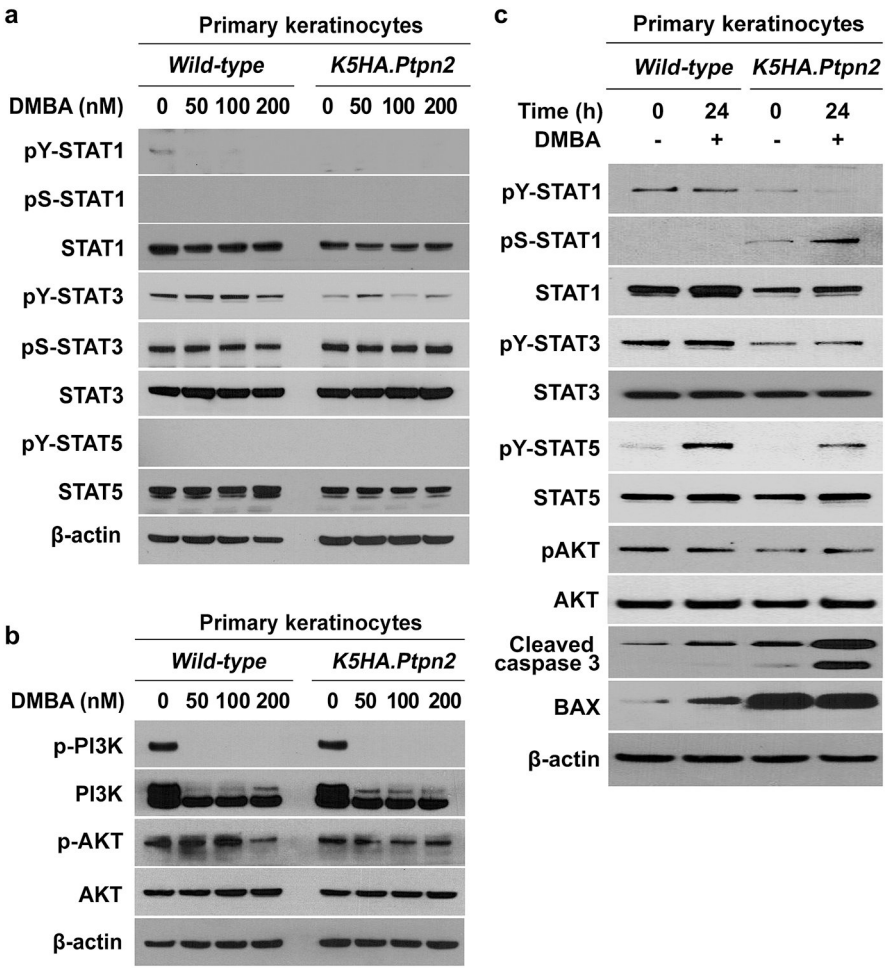

Figure 3. TC-PTP overexpression sensitizes DMBA-induced apoptosis through regulation of STAT and AKT signaling pathways.

a-b Primary keratinocytes from wild-type and *K5HA.Ptpn2* mice were cultured and treated with DMBA (50, 100, 200 nM). Following the 1 h pulse treatment of DMBA, cells were cultured for 1 h and total cell lysates were prepared. **a** Western blot analysis of p-STAT1, p-STAT3, p-STAT5 in primary keratinocytes from both genotypes after DMBA treatment. **b** Western blot analysis of p-PI3K and p-AKT in primary keratinocytes from both genotypes after DMBA treatment. **c** Primary keratinocytes from wild-type and *K5HA.Ptpn2* mice were cultured and treated with DMBA (100 nM). Western blot analysis of p-STAT1, p-STAT3, p-STAT5, p-AKT, Bax in primary keratinocytes from both genotypes after DMBA treatment (100 nM).

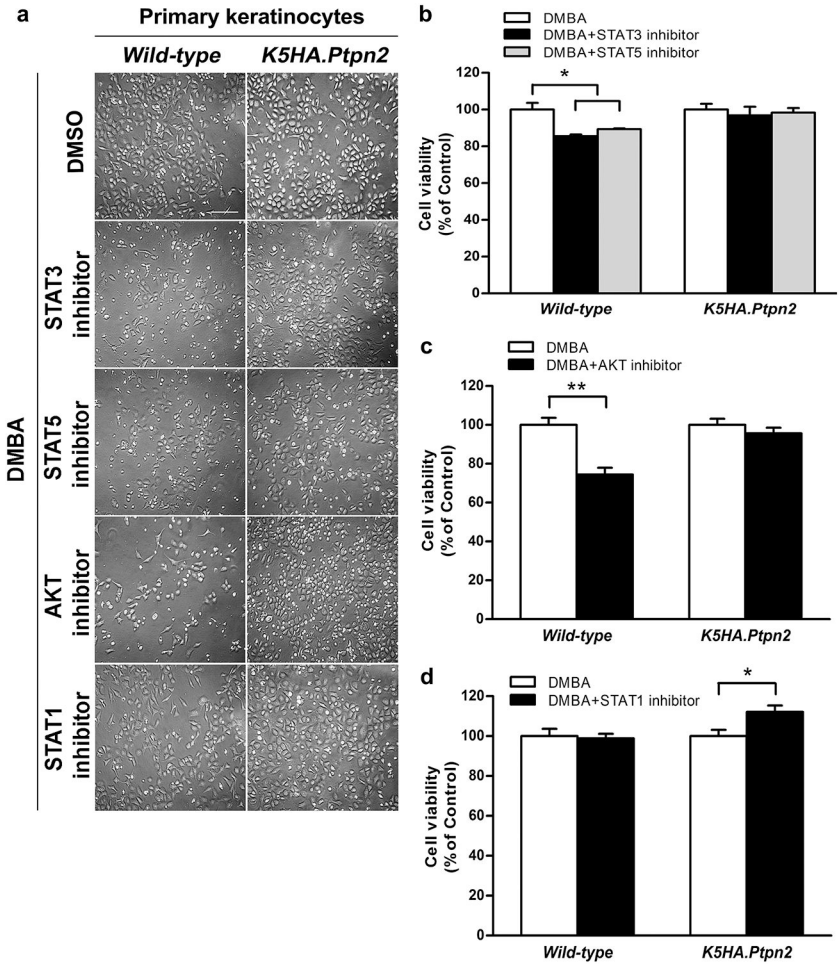

Figure 4. Inhibition of STAT1, STAT3, STAT5 or AKT on DMBA-induced apoptosis in keratinocytes.

a Representative photomicrographs of primary keratinocytes from wild-type and *K5HA.Ptpn2* mice. Primary keratinocytes from both genotypes were pretreated with STAT3 inhibitor STA21 (10 μM), STAT5 inhibitor N'-((4-Oxo-4h-chromen-3-yl)methylene)nicotinohydrazide (5 μM), AKT inhibitor A6730 (1 μM), or STAT1 inhibitor Fludarabine (10 μM) for 1 h before DMBA treatment (100 nM). Following the 1 h pulse treatment of DMBA, cells were cultured for 24 h. Scale bar: 100 μm. **b** Effect of inhibition of STAT3 or STAT5 on DMBA-induced apoptosis. Primary keratinocytes from both genotypes were pretreated with STAT3 inhibitor or STAT5 inhibitor for 1 h before DMBA treatment. Following the 1 h pulse treatment of DMBA, cell viability was measured after 24 h of DMBA treatment using WST-assay. *, $P < 0.05$ by ANOVA. **c** Effect of inhibition of AKT on DMBA-induced apoptosis. Primary keratinocytes from both genotypes were pretreated with AKT inhibitor for 1 h before DMBA treatment. Following the 1 h pulse treatment of DMBA, cell viability was measured after 24 h of DMBA treatment using WST-assay. **, $P < 0.01$ by ANOVA. **d** Effect of inhibition of STAT1 on DMBA-induced apoptosis. Primary keratinocytes from both genotypes were pretreated with STAT1 inhibitor for 1 h before DMBA treatment. Following the 1 h pulse treatment of DMBA, cell viability was measured after 24 h of DMBA treatment using WST-assay. *, $P < 0.05$ by ANOVA.

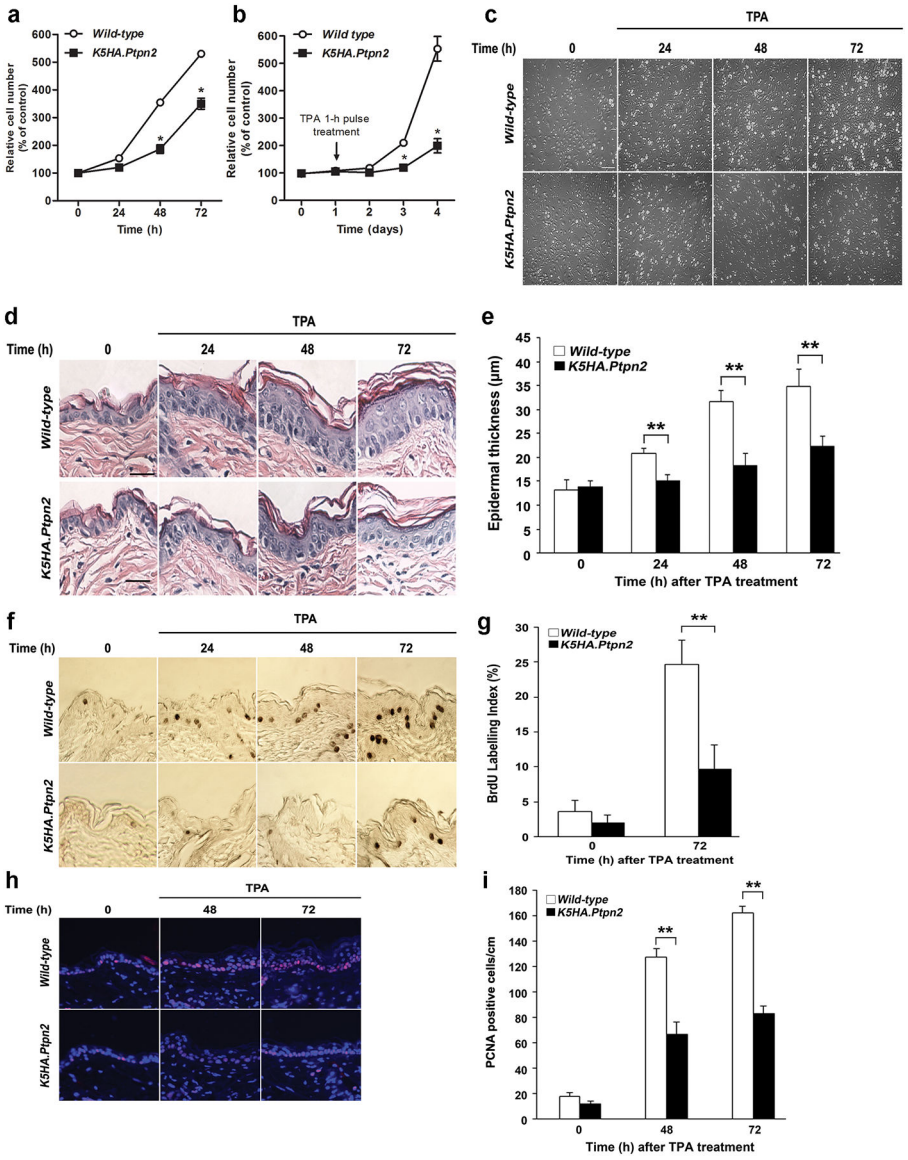

Figure 5. Effect of TC-PTP overexpression on epidermal hyperproliferation induced by TPA.

a Equivalent number of primary keratinocytes from wild-type and *K5HA.Ptpn2* mice were seeded and cultured for 72 h. Proliferation of primary keratinocytes was measured using the WST-assay. *, $P < 0.05$ by Mann-Whitney U test. Results are the mean ± s.d.m. **b** Primary keratinocytes were treated with TPA (50 nM) for 1 h. Proliferation of primary keratinocytes was measured using WST-assay. *, $P < 0.05$ by Mann-Whitney U test. Results are the mean ± s.d.m. **c** Representative photomicrographs of primary keratinocytes from both genotypes at 24 h, 48 h and 72 h after 50 nM of TPA treatment for 1 h. Scale bar: 100 μm. **d-i** Groups of mice (n=3/group) were treated topically with single application of TPA (6.8 nmol) and sacrificed 24, 48, 72 h after treatment. **d** Representative H&E staining of epidermis from both genotypes of mice. Scale bar: 50 μm. **e** Quantification of epidermal thickness from both genotypes treated with TPA. **, $P < 0.01$ by Mann-Whitney U test. **f** Representative BrdU staining of epidermis from both genotypes of mice. Scale bar: 100 μm. **g** Quantification of

BrdU-labled keratinocytes from epidermis of both genotypes. **, $P < 0.01$ by Mann-Whitney U test. **h** Representative PCNA staining of epidermis from both genotypes of mice. Scale bar: 100 μm. **i** Quantification of PCNA-positive keratinocytes from epidermis of both genotypes. **, $P < 0.01$ by Mann-Whitney U test.

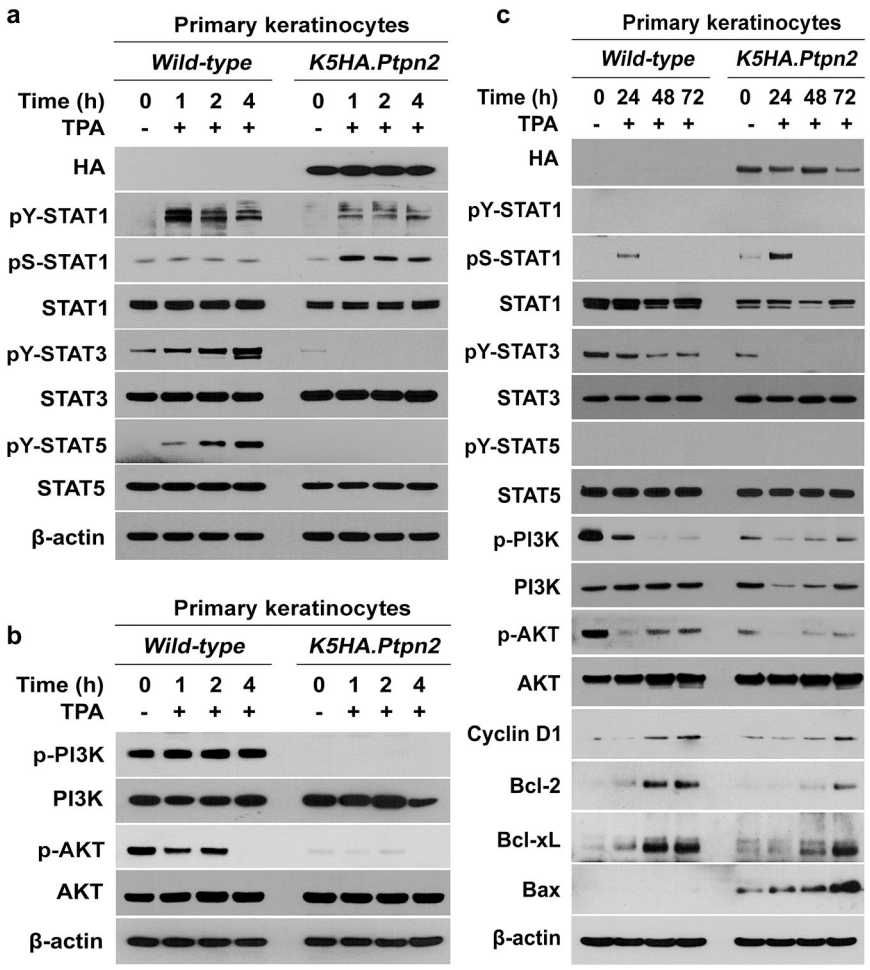

Figure 6. Overexpression of TC-PTP in epidermis reduces TPA-induced cell proliferation and survival through the regulation of STAT1, STAT3, STAT5, and PI3K/AKT signaling.

a-c Primary keratinocytes from wild-type and *K5HA.Ptpn2* mice were cultured and collected at the indicated time after TPA treatment (50 nM) and total cell lysates were prepared. **a** Western blot analysis of p-STAT1, p-STAT3, p-STAT5 in primary keratinocytes from both genotypes after TPA treatment. **b** Western blot analysis of p-PI3K and p-AKT in primary keratinocytes from both genotypes. **c** Western blot analysis of p-STAT1, p-STAT3, p-STAT5, p-PI3K, p-AKT, cyclin D1, Bcl-2, Bcl-xL, Bax in primary keratinocytes from both genotypes after TPA treatment.

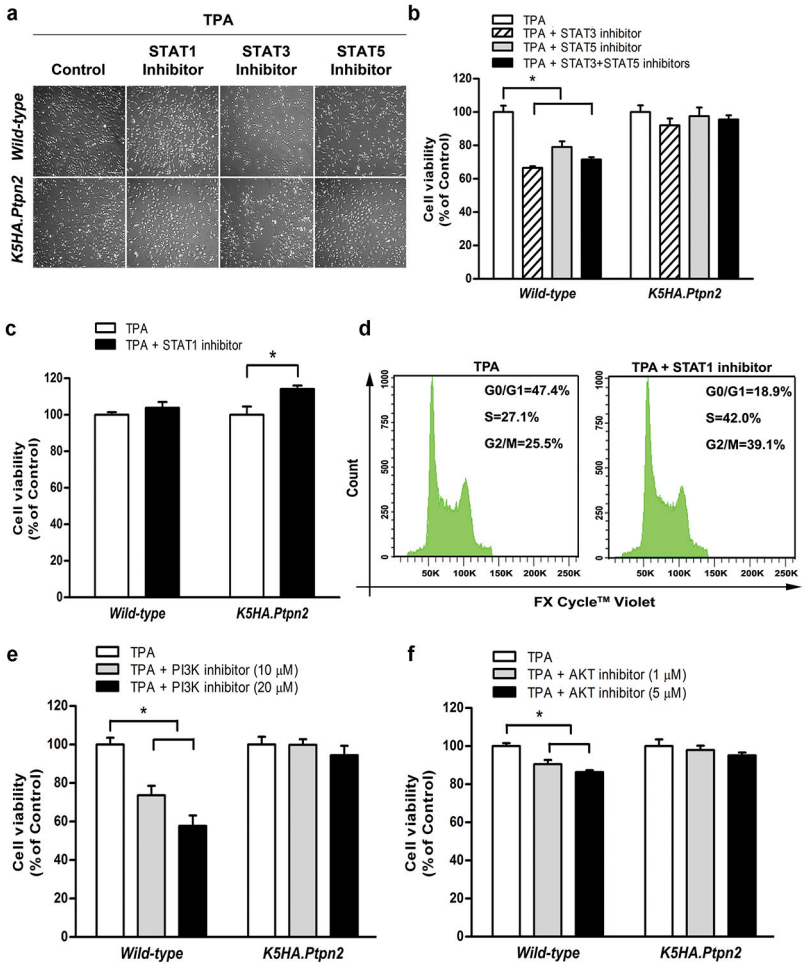

Figure 7. Inhibition of STAT1, STAT3, STAT5, PI3K, or AKT on TPA-induced keratinocyte survival and proliferation.

Primary keratinocytes from wild-type and *K5HA.Ptpn2* mice were pretreated with STAT1 inhibitor Fludarabine (10 μM), STAT3 inhibitor STA21 (10 μM), STAT5 inhibitor N'-((4-Oxo-4h-chromen-3-yl)methylene)nicotinohydrazide (10 μM), PI3K inhibitor LY294002 (10–20 μM), AKT inhibitor A6730 (1–5 μM) for 1 h before TPA treatment. Results are the mean ± s.d.m. **a** Representative morphological changes of primary keratinocytes from both genotypes following treatment of TPA for 24 h. Scale bar: 100 μm. **b** Quantitative analysis of percentage of viable cells after 24 h of TPA treatment. Primary keratinocytes from both genotypes were pretreated with STAT3 inhibitor and/or STAT5 inhibitor for 1 h before TPA treatment. Following the 1 h pulse treatment of TPA, cell proliferation was measured after 24 h of TPA treatment using WST-assay. *, $P < 0.05$ by ANOVA. **c** Quantitative analysis of cell viability after 24 h of TPA treatment. Primary keratinocytes from both genotypes were pretreated with STAT1 inhibitor for 1 h before TPA treatment. Following the 1 h pulse treatment of TPA, cell proliferation was measured after 24 h of TPA treatment using WST-assay. *, $P < 0.05$ by ANOVA. **d** Cell cycle analysis after 24 h of TPA treatment. Primary keratinocytes from *K5HA.Ptpn2* mice were pretreated with STAT1 inhibitor for 1 h before TPA treatment. Cell cycle analysis was performed by flow cytometry after 24 h of TPA treatment. **e-f** Effect of inhibition of PI3K or AKT on TPA-induced cell proliferation in

keratinocytes. Primary keratinocytes from both genotypes were pretreated with either (**e**) PI3K inhibitor LY294002 or (**f**) AKT inhibitor A6730 for 1 h before TPA treatment. Following the 1 h pulse treatment of TPA, cell proliferation was measured after 24 h of TPA treatment using WST-assay. *, $P < 0.05$ by ANOVA.

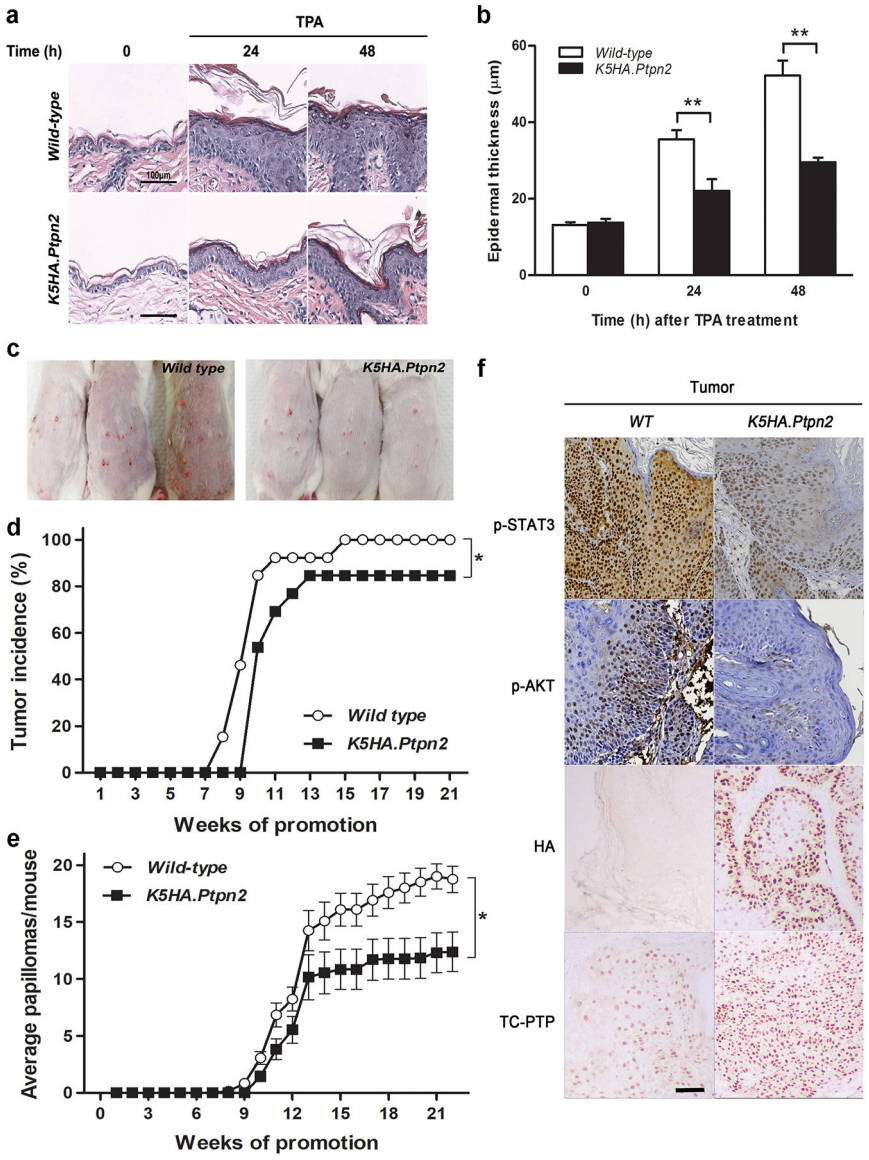

Figure 8. TC-PTP overexpression reduces tumor formation in the epidermis during two-stage skin carcinogenesis.

a Representative H&E staining of epidermis from wild-type and *K5HA.Ptpn2* mice. Both genotypes of mice were treated with twice-weekly application of 6.8 nmol of TPA for 2 weeks. Scale bar: 100 μm. **b** Quantification of epidermal thickness from both genotypes treated with TPA. **, $P < 0.05$ by Mann-Whitney *U* test. **c-e** Groups of from wild-type and *K5HA.Ptpn2* mice (n=13/group) were treated with 25 nmol DMBA and after 2 weeks treated with twice-weekly application of 6.8 nmol of TPA for the duration of the experiment. **c** Representative photograph of both genotypes of mice at the 21st week of tumor promotion. **d** Percentage of mice with tumors. *, $P < 0.05$ by Likelihood Ratio test. **e** Average number of tumors per mouse. (mean ± s.e.m.). *, $P < 0.05$ by Mann-Whitney *U* test. **f** Representative immunohistochemical staining of p-STAT3, p-AKT, HA, and TC-PTP in papillomas from both genotypes. Scale bar: 20 μm.

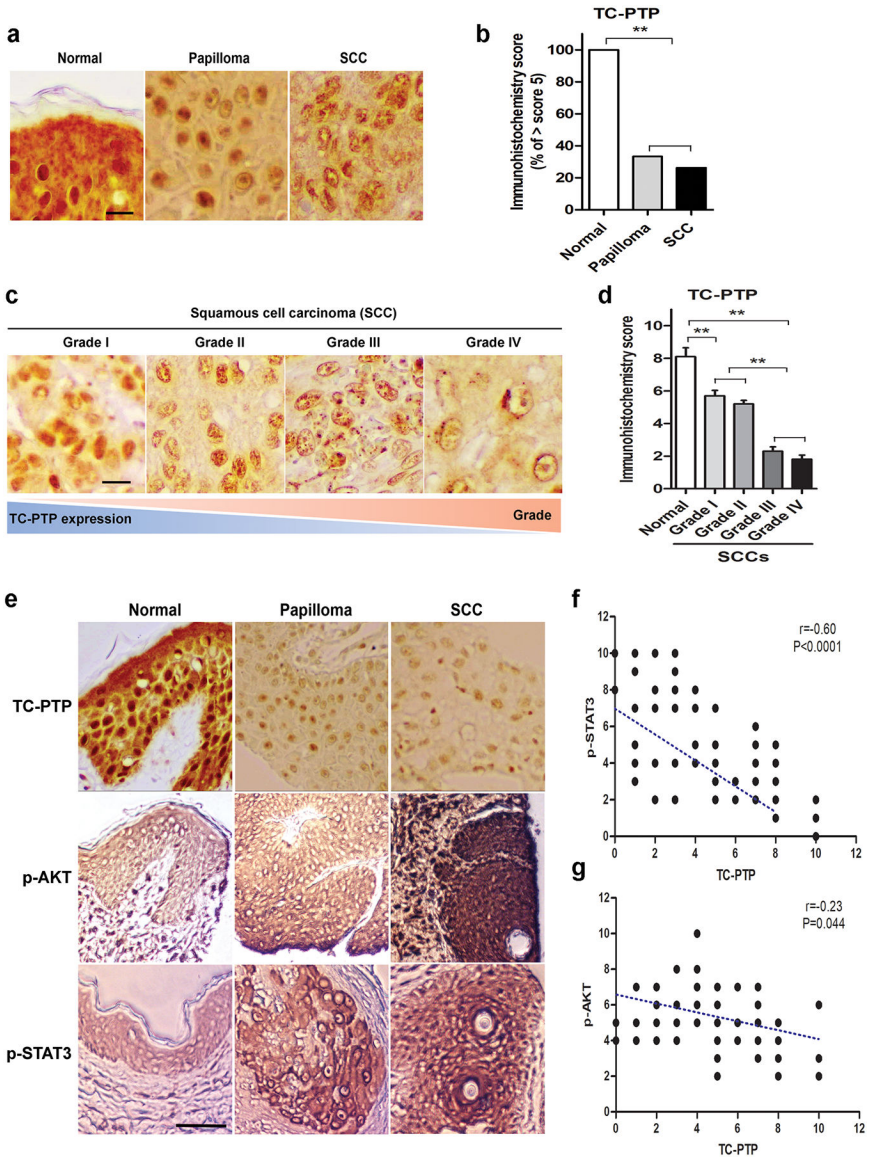

Figure 9. TC-PTP expression in human skin tumors.

a Representative immunohistochemical staining of TC-PTP in normal human skins (n=13), papillomas (n=6), and squamous cell carcinomas (SCCs) (n=57). Scale bar: 5 μm. **b** Quantification of TC-PTP expression by immunohistochemistry (IHC) scoring. Percentage of cells showing more than IHC score 5. TC-PTP expression levels from each of section were assessed as described in Methods. **, $P < 0.01$ by Mann-Whitney U test. **c** Representative immunohistochemical staining of TC-PTP in different grades of SCCs. Scale bar: 5 μm. **d** Quantification of TC-PTP expression by immunohistochemistry scoring. **, $P < 0.01$ by Mann-Whitney U test. **e** Representative immunohistochemical staining of TC-PTP, p-STAT3, and p-AKT in normal human skins, papillomas, and SCCs. Scale bar: 20 μm. **f-g** Correlation scatter plots for expression of TC-PTP, p-STAT3, and p-AKT in human skin tumors. The Pearson correlation coefficient was calculated with a two-tailed p value. **f**

Correlation between TC-PTP and p-STAT3 expression. r= −0.60, $P < 0.0001$. **g** Correlation between TC-PTP and p-AKT. r= −0.23, $P = 0.044$.